**RESEARCH**

# Crystal structure, packing features, DFT evaluation of intermolecular hydrogen bonds, and crystal lattice energy of a polymorph of 4-oxo-4-phenylbutanoic acid

Vyacheslav S. Grinev[1,2] · Anna E. Sklyar[1] · Ilya A. Demeshko[1] · Anastasia A. Lobankova[1] · Nikita A. Barabanov[1] · Alevtina Yu. Yegorova[1]

## Abstract

Different crystal forms of pharmaceutically important compounds demonstrate non-equivalent physical properties and, thus, bioactivity. Taking into consideration the polymorphism is crucial for many applications due to the prominent variation in properties of solids of the same chemical substance but with different crystal packing. The structure of 4-oxo-4-phenylbutanoic acid, $C_{10}H_{10}O_3$, at 120 K has monoclinic ($P2_1/c$) symmetry and is a $Z=8$, $Z'=2$ polymorph (γ-form). The previously published two polymorphs with CCDC codes VERMAG (α-form) and VERMAG01 (β-form) crystallize with $Z=4$, $Z'=1$ in the monoclinic space groups $P2_1/c$ [$a=15.071$ (10), $b=5.435$ (9), $c=16.058$ (10), $\beta=129.57$ (10)°] and $P2_1/n$ [$a=12.728$ (6), $b=5.200$ (3), $c=14.426$ (6), $\beta=111.33$ (3)°], respectively. Reported herein polymorph has a significantly larger cell volume of 1754.51 Å$^3$ [$a=15.2673$ (6), $b=5.2028$ (2), $c=22.3063$ (8), $\beta=98.0217$ (7)°]. Structurally, the γ-form differs from the two other known (RMSD does not exceed 0.2 Å). Only reported herein polymorph contains weak attractive C7—H7A···O3A close contacts between two neighboring molecules, giving some structural variety of the two crystallographically independent molecules as well as slight non-coplanarity between their phenyl rings. The previously reported polymorphs demonstrate carbonyl groups at position 4 unaffected. All polymorphs contain dimers of molecules bounded by two equivalent intermolecular hydrogen bonds. Investigation of three polymorphs of 4-oxo-4-phenylbutanoic acid highlights the importance of understanding the relationship between various parameters such as packing density, presence of different interactions within the crystal, and energy of the crystal lattice. This is of great importance for the development of new materials with specific physical properties and applications in various fields of science and technology, such as dyes and pigments, high-energy materials, and pharmaceuticals.

**Keywords** 4-oxo-4-phenylbutanoic acid · β-benzoylpropionic acid · Polymorph · Polymorphism · Hydrogen bonds · Hirshfeld surface analysis · DFT calculations · Hydrogen bond energy

## Introduction

Different crystal forms of pharmaceutically significant compounds demonstrate non-equivalent physical properties and, thus, bioactivity [1, 2]. Polymorphism is a phenomenon in which the same chemical substance can form various crystalline structures [3]. Also, worth mentioning is the importance of having the same stoichiometry for polymorphic forms. Taking into consideration the polymorphism is crucial for many applications due to the prominent variation in properties of solids of the same chemical substance but with different crystal packing [4–6].

4-Oxo-4-arylbutanoic acids, also known as β-benzoylpropionic acids, are crucial and convenient starting compounds for building various biologically active five-membered heterocycles such as furan-2(3H)-ones, pyrrolones [7], oxadiazoles, and triazoles [8], which have anti-inflammatory, analgesic, antimicrobial, and antiviral activity.

✉ Vyacheslav S. Grinev
grinevvs@sgu.ru

1 Institute of Chemistry, N.G. Chernyshevsky Saratov National Research State University, Saratov 410012, Russian Federation

2 Institute of Biochemistry and Physiology of Plants and Microorganisms, Saratov Scientific Centre of the Russian Academy of Sciences, 13 Prospekt Entuziastov, Saratov 410049, Russian Federation

In the early 1990s of the twentieth century, two works published detailed the characteristics of two distinct polymorphs of 4-oxo-4-phenylbutanoic acid. These works were deposited in the CCDC with the codes VERMAG (hereinafter referred to as α-form) and VERMAG01 (hereinafter referred to as β-form), correspondingly [9, 10]. The crystal of the first one, α-form, was obtained from methanol, while the second modification, β-form, was crystallized in benzene. Both polymorphs crystallize in monoclinic space groups, $P2_1/c$ (α-form) and the non-standard space group $P2_1/n$ (β-form), and have similar parameters of the crystal lattice. In 2018 [11], we very briefly reported the existence of a third polymorphic modification of 4-oxo-4-phenylbutanoic acid, hereinafter referred to as γ-form. Recently, there was a surge of attention in crystals of 4-oxo-4-phenylbutanoic acid again. The interest in the crystals of 4-oxo-4-phenylbutanoic acid has also been linked to their notably high coefficient of thermal expansion (2333.5 MK$^{-1}$), surpassing the average for organic crystals (168.8 MK$^{-1}$) [12]. Quite recently, 11 samples of crystals of 4-oxo-4-phenylbutanoic acid were obtained at higher temperatures (200–290 K), demonstrating the existence of two different structures with varying numbers of molecules in the asymmetric unit. It has been shown that up to 235 K, there are two molecules belonging to different phases in the crystal. The transition between two phases, the LT phase ($P2_1/c$) and the RT phase ($P2_1/n$), is assumed to occur at about 240 K. The gradual transition during cooling is tied to the emergence of pseudosymmetry [13]. The measured coefficient of volumetric thermal expansion, determined via high-resolution powder X-ray diffraction between 200 and 310 K, was αv = 217(3) MK$^{-1}$, aligning with typical values for organic substances. In the literature, there is also a mention of the crystal structure of 3-(4-methylbenzoyl)-propionic acid [14] and a short report about the crystal structure of 3-(4-methoxybenzoyl)-propionic acid [15], which differ from the titled compound by methyl and methoxy group, respectively, in benzene ring at the para-position. All mentioned crystals are Z′ = 1, which is the most common among them.

Today, scientists are paying great attention to crystals with Z′ ≥ 2. On the one hand, the disadvantage of crystals containing more than one independent molecule is that they exhibit lower symmetry [16]. On the other hand, there is an approach based on topological analysis of the experimental distribution of electron density. This approach allows one to investigate the response of the single molecule in crystals, with Z′ ≥ 2 to the surroundings [17] even when caused by weak interactions [18, 19]. The polymorph of 4-oxo-4-phenylbutanoic acid, with Z = 8 and Z′ = 2, reported here, also crystallizes in the $P2_1/c$ space group, but the parameters of the crystal lattice differ significantly from those of previously published crystals. Recently, there was a report about a special case of polymorphism at temperatures in the narrow 200–310 K range, and it was established that the single crystal may contain two phases of the titled compound [13]. In this work, we provide detailed information about the crystal investigated at 120 K with Mo irradiation which provides better resolution and gives more insight about the polymorphism of the titled compound. Herein, we report on a comparative analysis of the geometric parameters of 4-oxo-4-phenylbutanoic acid polymorphs as well as crystal packing features, in particular, Hirshfeld surface analysis, hydrogen bond energy evaluation, void analysis, and crystal lattice energy evaluation.

## Experimental

### Physical measurements

Elemental analysis was performed on a CHNS analyzer "Elementar Vario MICRO cube" (Elementar Analysensysteme GmbH, Germany). The melting point was determined on a *Stuart™ SMP10* melting point apparatus (Cole-Parmer, UK). FTIR spectra were recorded as KBr pellets on *Nicolet 6700 FTIR* spectrophotometer (Thermo Scientific, USA), in the 4000–400 cm$^{-1}$ range with a spectral resolution of 4 cm$^{-1}$. The $^1$H and $^{13}$C NMR spectra were recorded on a *Varian (Agilent)* 400 spectrometer (Agilent Technologies, Santa Clara, California, USA) with operating frequencies of 400 and 100 MHz, respectively, for solution in chloroform-*d* with TMS as an internal standard.

X-ray diffraction was performed on an automatic three-circle diffractometer *Bruker SMART Apex II* (graphite monochromator, λ(MoKα) = 0.71073 Å, ω scan) at 120 K. Integration of intensities was carried out using the procedure built into the software complex SAINT. Semi-empirical corrections for absorption and systematic errors are based on the intensity of equivalent reflections in the program SADABS.

### Synthesis and crystallization

4-Oxo-4-phenylbutanoic acid (**1**) was synthesized by Friedel-Crafts condensation from succinic anhydride and benzene with anhydrous AlCl$_3$ catalysis, recrystallized from water and dried under vacuum. M.p. 112–114 °C. Calculated, %: C, 67.41; H, 5.66 for C$_{10}$H$_{10}$O$_3$. Found, %: C, 67.38; H, 5.69. $^1$H NMR (400 MHz, chloroform-*d*): δ 10.77 (bs, 1H), 7.98 (d, J = 7.7 Hz, 2H), 7.58 (t, J = 7.4 Hz, 1H), 7.47 (t, J = 7.6 Hz, 2H), 3.32 (t, J = 6.6 Hz, 2H), 2.82 (t, J = 6.5 Hz, 2H); $^{13}$C NMR (100 MHz, chloroform-*d*) δ 197.82, 178.57, 136.35, 133.35, 128.65, 128.05, 33.15, 27.99. The single crystal of the titled compound for X-ray study was obtained from a hot benzene supersaturated solution followed by slow cooling to room temperature.

## Refinement

The structure was solved by a direct method and was refined by full-matrix least-squares versus $F^2$hkl with anisotropic displacement parameters for all non-hydrogen atoms [20]. The hydrogen atoms of the OH groups were found from the difference Fourier series and refined in the isotropic approximation. The other hydrogen atoms were placed in the calculated positions and were refined geometrically by using a riding model with $U_{iso}(H) = 1.2$ $U_{iso}(C)$ and $U_{iso}(H) = 1.5$ $U_{iso}(C)$. Solving and refinement were carried out using the SHELX software package version 2016/6 [21]. The overlays and packing diagrams as well as parameters of non-covalent interactions were obtained using Olex2 software [22]. Crystal data, data collection, and structure refinement details are summarized in Table 1. Reduced cell parameters were obtained using the Mercury 3.0 software structure information tool.

**Table 1** Experimental details

| | |
|---|---|
| Chemical formula | $C_{10}H_{10}O_3$ |
| $M$ | 178.18 |
| Crystal system, space group | Monoclinic, $P2_1/c$ |
| Temperature (K) | 120 |
| $a$, $b$, $c$ (Å) | 15.2673 (6), 5.2028 (2), 22.3063 (8) |
| $\beta$ (°) | 98.0217 (7) |
| $V$ (Å$^3$) | 1754.51 (12) |
| $Z$ | 8 |
| Radiation type | Mo$K\alpha$ |
| $\mu$ (mm$^{-1}$) | 0.10 |
| Crystal size (mm) | $0.31 \times 0.27 \times 0.23$ |
| Diffractometer | Bruker *SMART APEX* II diffractometer |
| Absorption correction | Multi-scan Bruker *SADABS* |
| No. of measured, independent, and observed [$I > 2\sigma(I)$] reflections | 22,469, 5417, 4496 |
| $R_{int}$ | 0.025 |
| $(\sin \theta/\lambda)_{max}$ (Å$^{-1}$) | 0.717 |
| Refinement | |
| $R[F^2 > 2\sigma(F^2)]$, $wR(F^2)$, $S$ | 0.040, 0.112, 1.04 |
| No. of reflections | 5417 |
| No. of parameters | 243 |
| H-atom treatment | H atoms treated by a mixture of independent and constrained refinement |
| $\Delta\rho_{max}$, $\Delta\rho_{min}$ (e Å$^{-3}$) | 0.36, −0.24 |

Computer programs: Bruker *APEX2* [23], Bruker *SAINT* [24], SHELXT [20], *SHELXL* [21], *SHELXTL* [24]

## DFT calculations

DFT calculations were performed using Gaussian 09 software [25] on a high-performance computing cluster of N.G. Chernyshevsky National Research Saratov State University. Coordinates from X-ray data were used as initial and full geometry optimization of monomers, and dimers were performed using B3LYP [26, 27], CAM-B3LYP [28], M06-2X [29], MPWB95 [30], WB97XD [31], and B97—D3 [32] functionals and the 6-311++G(3$df$,3$pd$) basis set. The nature of stationary points found was confirmed by Hessian analysis by the absence of imaginary frequencies. The total energy gains were calculated as a difference between the energy of the dimer and the doubled energy of the corresponding monomer.

Crystal lattice energies of all polymorphs were calculated using Crystal Explorer 21.5 software with CE-B3LYP/6-31G($d,p$) approach. The clusters for each of the polymorphs crystals were constructed using a radius of 20 Å according to Thomas et al. [33]. The crystal lattice energy in kJ/mol was calculated as the sum for the selected central molecule, being obtained as one-half of the product of the $N$ and $E_{tot}$ values. For our polymorph with $Z' = 2$ lattice energy, values were calculated for each crystallographically independent molecule separately and obtained as a mean value.

## Results and discussion

### Molecular structure of the γ-form

The content of the asymmetric unit, along with atom labeling, is presented in Fig. 1a. This structure has been deposited in the Cambridge Crystallographic Data Centre with the deposition number CCDC 1892013. These data can be obtained free of charge via https://www.ccdc.cam.ac.uk/structures/. Structurally, the reported here polymorphic modification of 4-oxo-4-phenylbutanoic acid differs very slightly from the previously mentioned modifications of crystals α-form and β-form (the RMS value is about 0.112–0.183 Å). The unit cell of the reported crystal contains four pairs of crystallographically independent molecules ($Z = 8$, $Z' = 2$) with RMSD of 0.241 Å (with inversion) (Fig. 1b). An interesting fact is that, according to the RMSD values, two crystallographically independent molecules reported here in crystal **1** differ from each other structurally more significantly than the molecules from all known polymorphs (Fig. 1c).

The first molecule is more planar, C2, C3 atoms and C4—O3 carbonyl group lie almost in one plane with an aromatic ring (the C5—C4—C3—C2 torsion angle of −179.24 (8)°), while the second crystallographically independent molecule is twisted (with corresponding C5A—C4A—C3A—C2A
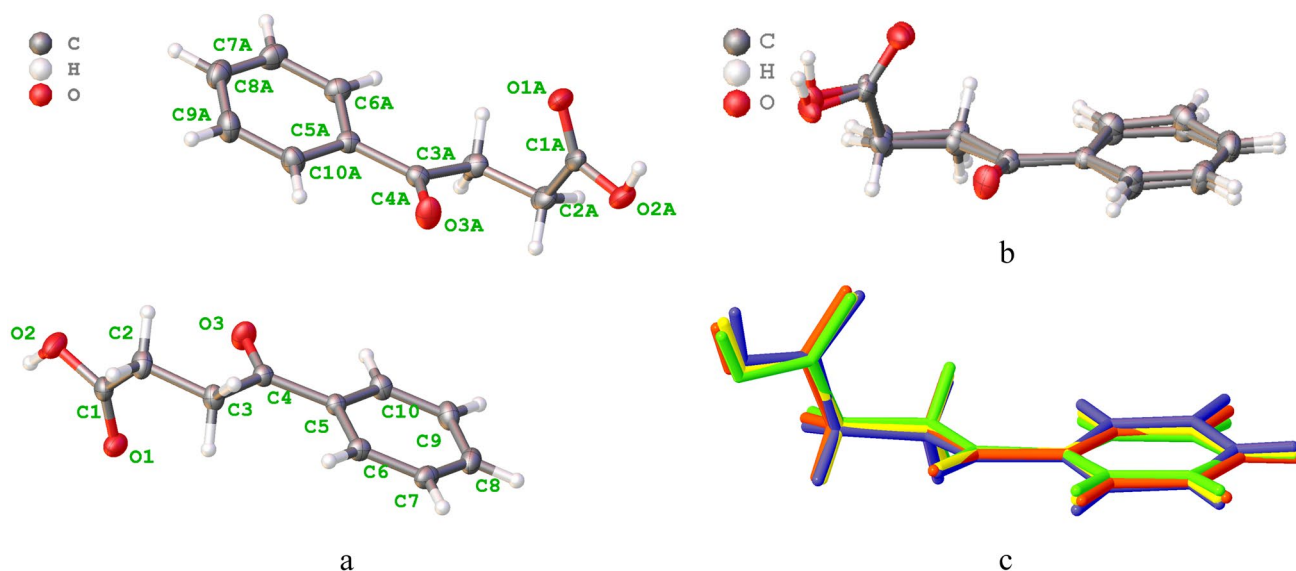
**Fig. 1** Geometry of 4-oxo-4-phenylbutanoic acid in γ-form. Displacement ellipsoids are drawn at the 50% probability level (**a**); overlapping diagrams of two crystallographically independent molecules in the crystal of γ-form (**b**); all four molecules; green—more "flat" molecule in γ-form, blue—"twisted" molecule in γ-form, orange—α-form, yellow—β-form (**c**)

torsion angle of 173.84 (8)°) even more than molecules of two polymorphs (corresponding torsion angles are[c] −177.9 (4)° and −176.2 (8)° for α- and β-forms, respectively). The phenyl rings of two independent molecules are not coplanar, which can be illustrated by two plane-to-plane angles, namely, a twist angle of 7.50 (4)° and a fold angle of 6.55 (3)°. The reason for observed structural differences between two crystallographically independent molecules as well as their non-coplanarity may lie in close contacts C7—H7A···O3A between two neighboring molecules, which was not implemented in crystals of α-form and β-form, where carbonyl groups at position 4 were not involved in such interactions. Such significant structural differences between crystallographically independent molecules resonate with the idea of the importance of $Z' = 2$ crystals to investigate subtle variations in the geometry of molecules depending on their surroundings [17–19].

All polymorphs contain dimers of molecules bounded by intermolecular hydrogen bonds between carboxyl groups. The summarized H-bond data for all considering crystals are given in Table 2. It can be seen that the H···O distances

in our crystal differ only by 0.036 Å, while the differences between this structure and α-form as well as β-form significantly more, and are 0.179 and 0.108 Å, correspondingly. It is noted that the H···O distance of the studied crystal of 4-oxo-4-phenylbutanoic acid lies in between α- and β-forms. The D···A distances of two molecules in the studied crystal as well as in the β-form polymorph are very similar (about 2.65 Å), in contrast with the α-form where this distance is about 0.1 Å longer.

## Crystal packing features of the γ-form

The reported monoclinic crystal of 4-oxo-4-phenylbutanoic acid belongs to the space group $P2_1/c$ (Fig. 2a–c). Selladurai et al. reported their structure (α-form) as a monoclinic crystal of the space group $P2_1/c$ with a $\beta$ angle of 129.57 (10)°, while Thompson et al. refined their structure (β-form) in the space group $P2_1/n$ with the less-obtuse $\beta$ angle of 111.33 (3)°. To the best of our knowledge, more accurate results can be achieved when using $P2_1/c$ for angles near 90°. So, our structure was refined in the

**Table 2** Hydrogen bond geometry (Å, °) of γ-form in comparison with other known polymorphs

| Polymorph | $D$—H···$A$ | $D$—H | H···$A$ | $D$···$A$ | $D$—H···$A$ |
|---|---|---|---|---|---|
| γ-Form (1) | O2—H2···O1[i] | 0.880 (19) | 1.778 (19) | 2.6560 (11) | 175.2 (18) |
| γ-Form (2) | O2A—H2O···O1A[ii] | 0.920 (19) | 1.742 (19) | 2.6550 (12) | 171.3 (17) |
| VERMAG (α-form) | O(2)—H(2a)···O(3)[iii] | 0.820 (1) | 1.939 (2) | 2.755 (3) | 173.200 (8) |
| VERMAG01 (β-form) | O(3)—H(10)···O(2)[iv] | 0.999 (3) | 1.652 (3) | 2.650 (4) | 176.56 (19) |

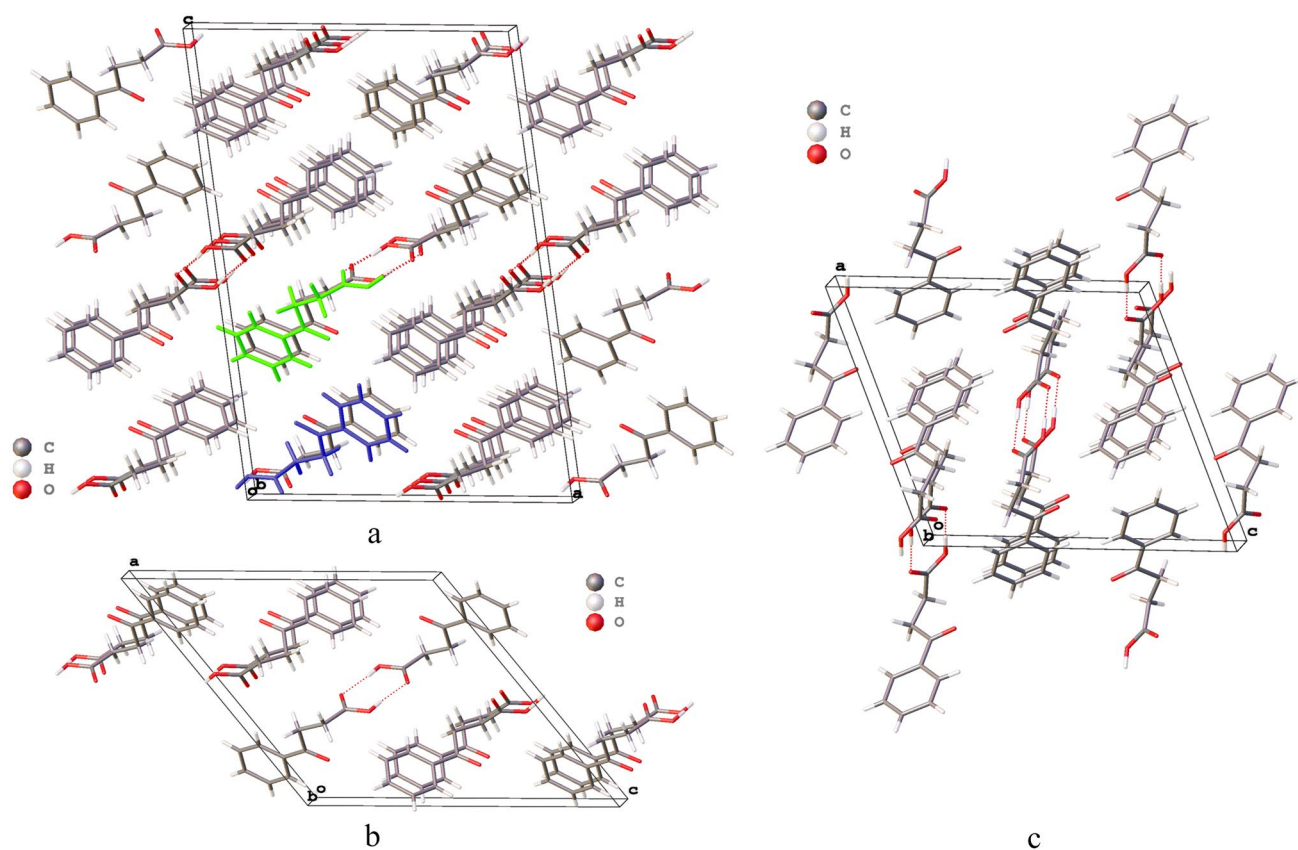Symmetry codes: (i) −x + 1, −y, −z + 1; (ii) −x, −y, −z; (iii) x, 1 + y, z; (iv) x, 1 + y, z

**Fig. 2** Packing diagrams showing the presence of intermolecular hydrogen bonds (the view along *b* axis) in the crystal of: γ-form. More "flat" molecule highlighted green, "twisted" molecule highlighted blue (**a**); α-form (**b**); β-form (**c**)

space group $P2_1/c$ with a sharper $\beta$ angle of 98.0217 (7)°. Obtained by using Mercury 3.0, reduced cell parameters were as follows: α-form (5.435, 13.2915, 15.071, 111.363, 90, 90), β-form (5.2, 12.728, 14.426, 111.33, 90, 90), and γ-form (5.2028, 15.2673, 22.3063, 98.0217, 90, 90). A comparison of parameters of reduced cells of all polymorphs revealed more pronounced similarities between α-form and β-form rather than between γ-form and the other form. The most significant difference is the value of $\alpha$ cell angle in γ-polymorph (98.0217°) in contrast to corresponding values in α- or β-form of approximately 111.3°.

The main difference between the three polymorphs is in the crystal packing. Briefly, the crystal package of α-form with a volume cell of 1013.91 Å$^3$ is intermediate, while β-form has a relatively compact unit cell with a volume of 889.4Å$^3$. The reported γ-form has the largest cell volume of 1754.51 Å$^3$ and two sets of molecules in comparison to early known modifications. Considering this, one can notice that the cell volume of the polymorph is twofold larger, in comparison to the β-polymorph, exactly due to the presence of two sets of crystallographically independent molecules.

## Hirshfeld surface analysis

To visualize the presence or the absence of close contacts in crystals of γ-form and α-form as well as β-form graphically, we performed an analysis of the Hirshfeld surface [34]. Hirshfeld surface analysis helps to investigate many areas of solid-state chemistry including intermolecular interactions and polymorphism. Hirshfeld surface analysis was performed using Crystal Explorer 21.5 [35]. The Hirshfeld surface diagrams, $d_{norm}$, with transparency, indicate, in red, the locations of the strongest intermolecular contacts, e.g., the H2A and H2AA atoms, which are important for intermolecular hydrogen bonding. The Hirshfeld surface diagrams reported herein polymorph γ-form as well as other known crystals are shown in Fig. 3a–d.

The main contribution to the Hirshfeld surface makes H···H intermolecular interactions in all polymorphs with values in the 38.0–38.5% range. The contributions of the other major intermolecular interactions in the crystal of γ-form are as follows: O···H (18.3%), C···H (14.0%), H···O (15.6%), and H···C (11.7%). Other contacts including C···C ones, which represent commonly π···π interactions, are less than or equal to 1% which is not significant. The

**Fig. 3** The Hirshfeld surface diagram ($d_{norm}$) for the asymmetric units of the crystals. The surface regions with the strongest intermolecular interactions are drawn in red color. Highlighted C7—H7A···O3A interaction in crystal of γ-form (**a**); γ-form (**b**); α-form (**c**); β-form (**d**)
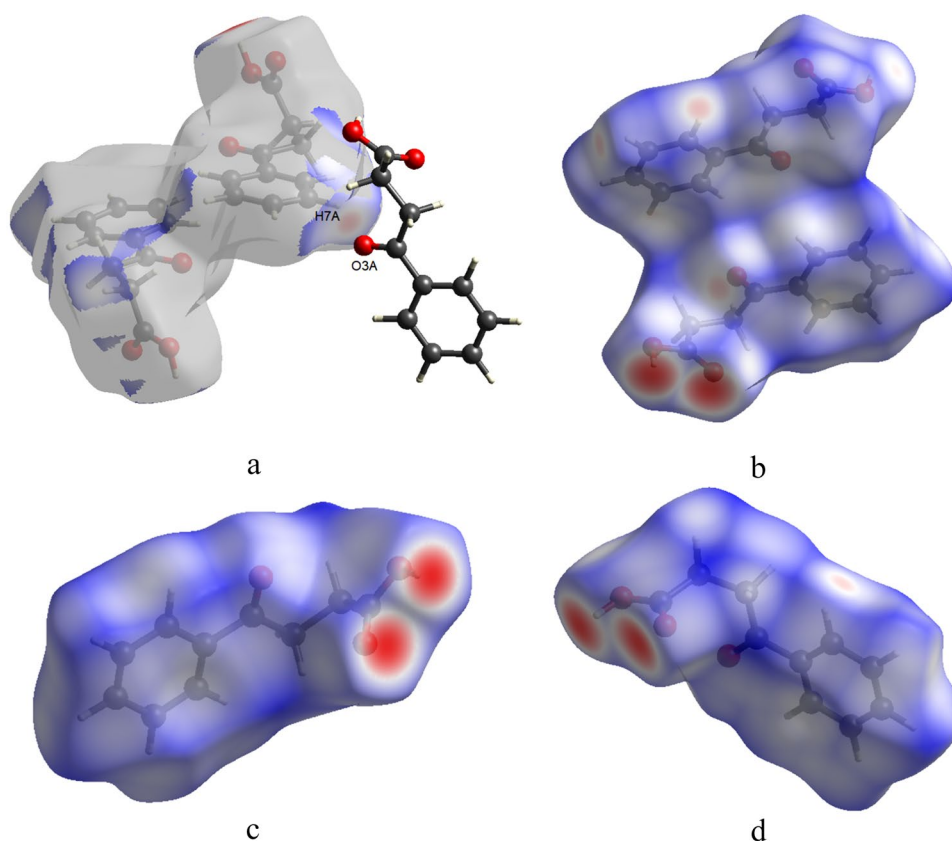


O···H/H···O contacts represent hydrogen bonds as well as the C7—H7A···O3A interaction between two neighboring molecules (Fig. 3a). Summarized contribution of these contacts in γ-form is slightly less than in both reported previously polymorphs that could be just a reflection of different parameters during the refinement procedure. The C···H/H···C contacts are pronounced more than in both other polymorphs, and, by nature, they are the H···π interactions of both aliphatic and aromatic H-atoms. This correlates with more dense packing in γ-form in comparison with other polymorphs.

The H···H, H···O, and H···C contributions to the crystal packing are shown as a Hirshfeld surface two-dimensional fingerprint plot with blue dots. The $d_e$ (y axis) and $d_i$ (x axis) values represent the closest external and internal distances (Å), correspondingly, from given points on the Hirshfeld surface contacts (Fig. S1a-l). The intermolecular hydrogen bonding, as well as Ph—C=O···H non-covalent interactions, are presented by the H···O/O···H contacts (33.9%) on a dotted diagram (Fig. S1g). Two sharp spikes with $d_e + d_i = \sim 1.65$ Å for H···O interatomic distance corresponding to H-bonds in dimers of both crystallographically independent molecules in the crystal of γ-form. The H···π interactions of both aliphatic and aromatic H-atoms (Fig. S1j) are represented by spread area with minimum $d_e + d_i = \sim 2.80$ Å for H···C.

## Void analysis

The mechanical strength of a single crystal is determined by how its constituent atoms are arranged within the crystal lattice. A crystal exhibiting minimal void volume can withstand significant levels of mechanical stress [36]. To determine the presence or absence of significant/cavities in the crystal of γ-form, Crystal Explorer 21.5 was utilized. Within the Crystal Explorer approach, the void surface is defined by generating an isosurface representing the electron density of the procrystal, which is then calculated for the entire unit cell with isovalue of 0.002 e a.u.$^{-3}$ and a standard void cluster of unit cell dimension $+5$ Å.

The density of the γ-form 1.349 Mg m$^{-3}$ is closer to the corresponding value of the β-form (1.331 Mg m$^{-3}$). The least dense form is the α-form (1.167 Mg m$^{-3}$).

Figure 4a and b depict graphical representations of the voids in the crystal packing of crystal γ-form, with a void volume of 147.98 Å$^3$. Additionally, the percentage of free space in the unit cell was calculated to be 8.43%. These findings suggest a compact arrangement of atoms within the crystal packing, indicating a high level of mechanical stability.

Regarding the α- and β-form polymorphs, their percentage void volumes are 18.56 and 9.68, respectively. Based on these values, it can be concluded that the newly studied
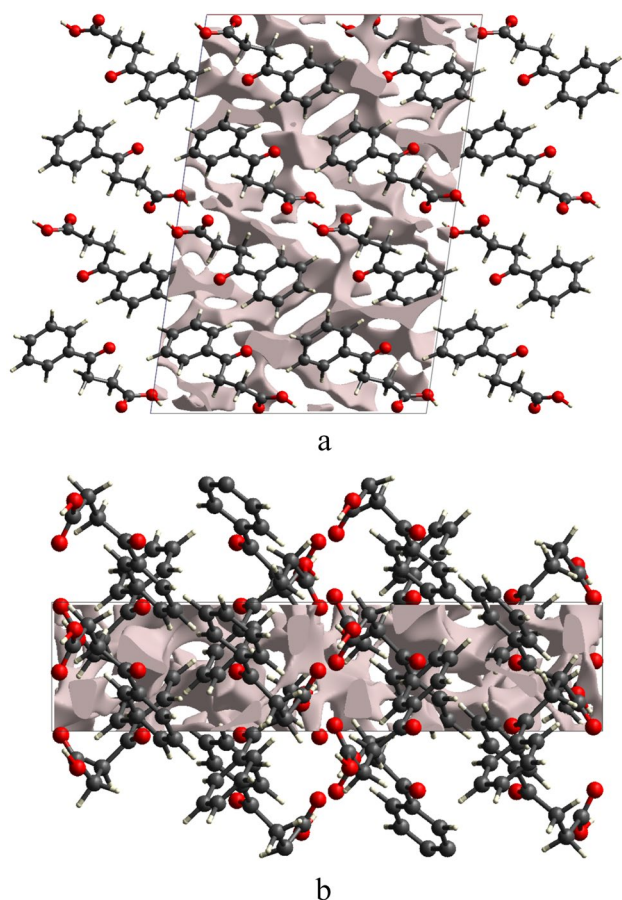
**Fig. 4** Diagram showing voids in the crystal of γ-form along *a* axis (**a**), along *b* axis (**b**)

polymorph of γ-form is a modification, containing the least relative amount of voids, compared to the previously known polymorphs, which aligns with the data on crystal packing, described above. The correlation between the percentage of void volume and the density of the crystal is clearly visible. When the volume of voids is less, then the density of the crystal is greater.

Considering all three known at-the-day crystals of 4-oxo-4-phenylbutanoic acid, γ-form has the densest package. In all known crystals, molecules of the acid are formed dimers using carboxyl groups which are in harmony with the common data for all carboxylic acids. The parameters of intermolecular hydrogen bonds of our crystal lie between corresponding values of known polymorphs and look ordinary.

## DFT calculations

To evaluate the energetics of the intermolecular hydrogen bonds in crystals of γ-form and both other polymorphs, DFT calculations were performed on the monomers and dimers of named molecules. The choice of the appropriate function in DFT is crucial for better accuracy of prediction. Many commonly used hybrid functionals like B3LYP describe well the geometry of the single molecule, but almost useless in the modeling of systems consisting of molecules connected by non-covalent interactions. Besides, the dimer as the system of a pair of identical molecules with two strongly pronounced hydrogen bonds is relatively simple for modeling even by functionals, which have no dispersion corrections. So, we have chosen some functionals, namely, B3LYP [26, 27], CAM-B3LYP [28], M06-2X [29], MPWB95 [30], WB97XD [31], and B97—D3 [32]. These functionals are frequently used for modeling non-covalent interacted systems with the large triple zeta 6-311++G($3df$,$3pd$) basis set. A criterion of the good prediction of the model was the reproduction of the geometry of hydrogen bonds as well as the general disposition of molecules in comparison to X-ray data. The obtained results are summarized in Table 3.

All functionals used gave very similar results describing the geometry of monomers and dimers of γ-form as well as both polymorphs. A common trend for all methods used is the flattening of D—H···A angle in dimers, which is the restriction of the dimeric model in a vacuum, while in crystals, dimers are surrounded by other molecules. Interatomic distances D···A were predicted in the 1.612–1.659 Å range which is slightly less than corresponding experimental

**Table 3** Calculated hydrogen bond geometry (Å, °) and energy[i] (kcal/mol) of γ-form in comparison with other known polymorphs

| Method[ii] | γ-Form | | | | VERMAG (α-form) | | | | VERMAG01 (β-form) | | | |
|---|---|---|---|---|---|---|---|---|---|---|---|---|
| | H···A | D···A | D—H···A | E | H···A | D···A | D—H···A | E | H···A | D···A | D—H···A | E |
| B3LYP | 1.658 | 2.658 | 179.52 | −15.59 | 1.659 | 2.659 | 179.49 | −15.59 | 1.659 | 2.659 | 179.50 | −15.60 |
| CAM-B3LYP | 1.629 | 2.630 | 179.61 | −17.69 | 1.629 | 2.630 | 179.60 | −17.68 | 1.628 | 2.629 | 179.63 | −17.68 |
| M06-2X | 1.627 | 2.626 | 179.39 | −17.51 | 1.624 | 2.625 | 179.57 | −17.40 | 1.626 | 2.624 | 179.41 | −17.41 |
| MPWB95 | 1.633 | 2.650 | 177.92 | −15.37 | 1.634 | 2.651 | 177.93 | −15.46 | 1.635 | 2.651 | 177.90 | −15.31 |
| B97D3 | 1.613 | 2.625 | 177.68 | −17.31 | 1.612 | 2.625 | 177.68 | −17.32 | 1.612 | 2.625 | 177.67 | −17.32 |
| WB97XD | 1.653 | 2.648 | 179.47 | −17.94 | 1.653 | 2.649 | 179.45 | −18.00 | 1.654 | 2.648 | 179.46 | −18.00 |
| | $E_{lattice}$ | | | | $E_{lattice}$ | | | | $E_{lattice}$ | | | |
| CE-B3LYP | −23.9 and −30.2 (average, −27.0) | | | | −26.6 | | | | −30.5 | | | |

values (1.652 (3)–1.939 (2) Å) due to systematic underestimation of such distances by DFT methods. The overall energy gains obtained by calculations as doubled hydrogen bond energy were in the 15.37–18.00 kcal/mol range, which gives ~ 7.65–9.00 kcal/mol per one H-bond, corresponding to relatively moderate strength hydrogen bonding.

Thus, our calculations revealed the relevancy of approximations used and confirmed the presence of strong intermolecular hydrogen bonds in crystals of all three polymorphs.

## Crystal lattice energy calculations

In order to compare the relative stability of all known polymorphs of 4-oxo-4-phenylbutanoic acid (**1**), DFT calculations of the energy of crystal lattice were performed using the Crystal Explorer 21.5 software and the CE-B3LYP/6-31G(*d,p*) approach [37]. This study investigated three known polymorphic modifications of **1** crystals with different packing densities. According to the calculation results, the reported crystal of **1** gave significantly different lattice energy values (−23.9 and −30.2 kcal/mol for two independent molecules, separately (Table 3)). For the whole crystal of **1**, the lattice energy should be believed as the mean value, −27.0 kcal/mol. Remarkably, the less dense α-form modification has almost the same energy as the lattice of −26.6 kcal/mol. The β-form modification has the lowest lattice energy of −30.5 kcal/mol among all three polymorphs. According to the data obtained, it can be assumed that the polymorphic modification studied by us is a kind of mixed-type crystal, which includes various forms of packing, energetically similar to the two known modifications, α- and β-forms. Comparing these three modifications, it can be concluded that packing density, percentage of voids, and the presence of intermolecular interactions have a significant connection with the lattice energy.

## Conclusion

Taking into consideration the polymorphism is crucial for many applications due to the prominent variation in properties of solids of the same chemical substance but with different crystal packing. Studying polymorphic modifications of 4-oxo-4-phenylbutanoic acid crystals with different packing densities and lattice energies provides valuable insights into the capabilities of molecules to form different arrangements within the crystal. Only reported herein polymorph contains weak attractive C7—H7A···O3A close contacts between two neighboring molecules giving some structural variety of the two crystallographically independent molecules as well as slight non-coplanarity between their phenyl rings. This may be an explanation for the denser packing molecules in the

crystal structure, which leads to relatively stronger interactions between molecules.

**Author contributions** V.S.G: conceptualization, data curation, validation, visualization, funding, resources, supervision, project administration, writing—original draft, writing—review and editing; A.E.S., I.A.D., A.A.L., N.A.B.: investigation, formal analysis, data collection, writing—original draft; A.Yu.Ye.: supervision. All authors reviewed the manuscript.

## Declarations

**Competing interests** The authors declare no competing interests.

## References

1. Ozturk II, Banti CN, Kourkoumelis N et al (2014) Synthesis, characterization and biological activity of antimony(III) or bismuth(III) chloride complexes with dithiocarbamate ligands derived from thiuram degradation. Polyhedron 67:89–103. https://doi.org/10.1016/j.poly.2013.08.052
2. Dubey R, Singh P, Singh AK et al (2014) Polymorphic signature of the anti-inflammatory activity of 2,2′-{[1,2-phenylenebis(methylene)]bis(sulfanediyl)}bis(4,6-dimethylnicotinonitrile). Cryst Growth Des 14:1347–1356. https://doi.org/10.1021/cg401842y
3. Cruz-Cabeza AJ, Reutzel-Edens SM, Bernstein J (2015) Facts and fictions about polymorphism. Chem Soc Rev 44:8619–8635. https://doi.org/10.1039/C5CS00227C
4. Goloveshkin AS, Korlyukov AA, Vologzhanina AV (2021) Novel polymorph of favipiravir—an antiviral medication. Pharmaceutics 13:139. https://doi.org/10.3390/pharmaceutics13020139
5. Drebushchak VA, McGregor L, Rychkov DA (2017) Cooling rate "window" in the crystallization of metacetamol form II. J Therm Anal Calorim 127:1807–1814. https://doi.org/10.1007/s10973-016-5954-0
6. McGregor L, Rychkov DA, Coster PL et al (2015) A new polymorph of metacetamol. CrystEngComm 17:6183–6192. https://doi.org/10.1039/C5CE00910C
7. Husain A, Khan MSY, Hasan SM, Alam MM (2005) 2-arylidene-4-(4-phenoxy-phenyl)but-3-en-4-olides: synthesis, reactions and biological activity. Eur J Med Chem 40:1394–1404. https://doi.org/10.1016/j.ejmech.2005.03.012
8. Hashem AI, Youssef ASA, Kandeel KA, Abou-Elmagd WSI (2007) Conversion of some 2(3H)-furanones bearing a pyrazolyl group into other heterocyclic systems with a study of their antiviral activity. Eur J Med Chem 42:934–939. https://doi.org/10.1016/j.ejmech.2006.12.032
9. Selladurai S, Kumar MS, Subramanian K (1990) Crystal and molecular structure of 3-benzoylpropionic acid. Proc Indian Acad Sci (Chem Sci) 102:39–43. https://doi.org/10.1007/BF02861569

10. Thompson HW, Vanderhoff PA, Lalancette RA (1991) 3-Benzo-ylpropionic acid: structure and hydrogen-bonding pattern. Acta Crystallogr C Cryst Struct Commun 47:1443–1445. https://doi.org/10.1107/S0108270190012173

11. Grinev V, Linkova E, Krivoshchekova E, Yegorova A (2018) A new 4-oxo-4-phenylbutanoic acid polymorph. In: The 1st international electronic conference on crystals. MDPI, p 1119. https://doi.org/10.3390/IECC_2018-05254

12. Van Der Lee A, Dumitrescu DG (2021) Thermal expansion properties of organic crystals: a CSD study. Chem Sci 12:8537–8547. https://doi.org/10.1039/D1SC01076J

13. Poręba T, Świątkowski M, Confalonieri G (2023) Melting pseudosymmetry and thermal expansion in 3-benzoylpropionic acid. CrystEngComm 25:5932–5941. https://doi.org/10.1039/D3CE00940H

14. Frey M, Harris SG, Holmes JM et al (2000) Elucidating the mode of action of a corrosion inhibitor for iron. Chem Eur J 6:1407–1415. https://doi.org/10.1002/(SICI)1521-3765(20000417)6:8%3c1407::AID-CHEM1407%3e3.0.CO;2-K

15. Ali S, Rama NH, Qadeer G, Ruzicka A (2008) 3-(4-Methoxy-benzoyl)propionic acid. Acta Crystallogr E Struct Rep Online 64:o2197–o2197. https://doi.org/10.1107/S1600536808034508

16. Ruck M (2000) Kristallographische Konsequenzen von Pseudosymmetrie in Kristallstrukturen. Z Kristallogr Cryst Mater 215:148–156. https://doi.org/10.1524/zkri.2000.215.3.148

17. Nelyubina YV, Barzilovich PYu, Antipin MYu et al (2011) Cation-π and lone pair-π interactions combined in one: the first experimental evidence of (H3O-lp)+···π-system binding in a crystal. ChemPhysChem 12:2895–2898. https://doi.org/10.1002/cphc.201100294

18. Nelyubina YV, Dalinger IL, Lyssenko KA (2011) Pseudosymmetry in trinitropyrazole: the cost of error in space-group determination. Angew Chem Int Ed 50:2892–2894. https://doi.org/10.1002/anie.201006000

19. Nelyubina YV, Antipin MYu, Cherepanov IA, Lyssenko KA (2010) Pseudosymmetry as viewed using charge density analysis. CrystEngComm 12:77–81. https://doi.org/10.1039/B912147A

20. Sheldrick GM (2015) *SHELXT* – integrated space-group and crystal-structure determination. Acta Crystallogr A Found Adv 71:3–8. https://doi.org/10.1107/S2053273314026370

21. Sheldrick GM (2015) Crystal structure refinement with SHELXL. Acta Cryst C 71:3–8. https://doi.org/10.1107/S2053229614024218

22. Dolomanov OV, Bourhis LJ, Gildea RJ et al (2009) OLEX2: a complete structure solution, refinement and analysis program. J Appl Crystallogr 42:339–341. https://doi.org/10.1107/S0021889808042726

23. Bruker (2009) APEX2, SAINT and SADABS. Bruker AXS Inc., Madison. References - Scientific Research Publishing. https://www.scirp.org/reference/referencespapers.aspx?referenceid=793779. Accessed 8 Oct 2023

24. Sheldrick GM (2008) SADABS, version 2008/1. Bruker AXS Inc., Madison. References - Scientific Research Publishing. https://www.scirp.org/reference/ReferencesPapers.aspx?ReferenceID=1912129. Accessed 8 Oct 2023

25. Frisch MJ, Trucks GW, Schlegel HB et al (2009) Gaussian 09 revision C 01 Gaussian 09 revis B01. Gaussian Inc., Wallingford. References - Scientific Research Publishing. https://www.scirp.org/reference/ReferencesPapers.aspx?ReferenceID=2085590. Accessed 8 Oct 2023

26. Becke AD (1988) Density-functional exchange-energy approximation with correct asymptotic behavior. Phys Rev A 38:3098–3100. https://doi.org/10.1103/PhysRevA.38.3098

27. Lee C, Yang W, Parr RG (1988) Development of the Colle-Salvetti correlation-energy formula into a functional of the electron density. Phys Rev B 37:785–789. https://doi.org/10.1103/PhysRevB.37.785

28. Yanai T, Tew DP, Handy NC (2004) A new hybrid exchange–correlation functional using the Coulomb-attenuating method (CAM-B3LYP). Chem Phys Lett 393:51–57. https://doi.org/10.1016/j.cplett.2004.06.011

29. Zhao Y, Truhlar DG (2008) The M06 suite of density functionals for main group thermochemistry, thermochemical kinetics, noncovalent interactions, excited states, and transition elements: two new functionals and systematic testing of four M06-class functionals and 12 other functionals. Theor Chem Acc 120:215–241. https://doi.org/10.1007/s00214-007-0310-x

30. Zhao Y, Truhlar DG (2004) Hybrid meta density functional theory methods for thermochemistry, thermochemical kinetics, and non-covalent interactions: the MPW1B95 and MPWB1K models and comparative assessments for hydrogen bonding and van der Waals interactions. J Phys Chem A 108:6908–6918. https://doi.org/10.1021/jp048147q

31. Remya K, Suresh CH (2013) Which density functional is close to CCSD accuracy to describe geometry and interaction energy of small noncovalent dimers? A benchmark study using Gaussian09. J Comput Chem 34:1341–1353. https://doi.org/10.1002/jcc.23263

32. Grimme S (2006) Semiempirical GGA-type density functional constructed with a long-range dispersion correction. J Comput Chem 27:1787–1799. https://doi.org/10.1002/jcc.20495

33. Thomas SP, Spackman PR, Jayatilaka D, Spackman MA (2018) Accurate lattice energies for molecular crystals from experimental crystal structures. J Chem Theory Comput 14:1614–1623. https://doi.org/10.1021/acs.jctc.7b01200

34. Hirshfeld FL (1977) Bonded-atom fragments for describing molecular charge densities. Theoret Chim Acta 44:129–138. https://doi.org/10.1007/BF00549096

35. Spackman PR, Turner MJ, McKinnon JJ et al (2021) *CrystalExplorer*: a program for Hirshfeld surface analysis, visualization and quantitative analysis of molecular crystals. J Appl Crystallogr 54:1006–1011. https://doi.org/10.1107/S1600576721002910

36. Segurado J, Llorca J (2009) An analysis of the size effect on void growth in single crystals using discrete dislocation dynamics. Acta Mater 57:1427–1436. https://doi.org/10.1016/j.actamat.2008.11.031

37. Mackenzie CF, Spackman PR, Jayatilaka D, Spackman MA (2017) *CrystalExplorer* model energies and energy frameworks: extension to metal coordination compounds, organic salts, solvates and open-shell systems. IUCrJ 4:575–587. https://doi.org/10.1107/S205225251700848X